URMC HEALTH LAB: HANDHELD ULTRASOUND SCANNING SYSTEM

Amanda Lee **Elizabeth Martin** **Leslii Silveus** **Ava Staub**

ABSTRACT

The objective of this project was to create a scanning apparatus that will improve the scanning process of the iQ3 Butterfly Ultrasound Probe (Figure 1.) for use with damaged finger tendons. This project was sponsored by the URMC Health Lab which had a prototype of this project already started. Based off the feedback from the prototype, a new design of the apparatus was created and used for the semester. After multiple iterations on various parts of the device, a prototype was put together to start testing with. The scanning mechanism has both a manual and automated part so the scanning can be done with a person controlling the movement of the probe or autonomously with the probe moving based on feedback from a laser sensor. All the programing was done using Arduinos and the Arduino IDE software. NX was used for all the CAD and analysis along with exporting components to be 3D printed. To test the code, a 3D printed hand was placed underneath the apparatus to make sure everything moved as expected. Once a water bath was constructed, it was placed underneath and testing could be done on actual finger tendons. Most of the requirements and specifications were met and it was decided that some aspects would be pushed back to the Health Lab to complete, such as the image processing components.

Figure 1. iQ3 Butterfly Probe.

PROBLEM DEFINITION

Ultrasound imaging is critical in diagnostics but is limited by two key challenges: it requires specialized expertise to operate and analyze, and traditional handheld probes are restricted to 2D imaging. In clinical settings for tendon repair therapy, there is no fully automated scanning system that can cohesively and accurately scan a damaged hand tendon, obtain 3D ultrasound images, calculate the scar tissue volume, and predict the functionality of the patient's tendon. Developing a device that automates ultrasound scans using handheld probes, while safely preventing contact with the patient's injured hand, will improve image quality, diagnostic accuracy, and patient comfort.

DELIVERABLES, REQUIREMENTS, SPECIFICATIONS

TABLE 1
DELIVERABLES

Deliverables	
1	Prototype mount compatible with phone and butterfly
2	Prototype water tank for patient's arm/hand
3	Prototype scanning device
4	Prototype software to support prototypes movement
5	Design report to include in testing
6	Complete CAD and bill of materials
7	Prototype software for image processing

TABLE 2
REQUIREMENTS

Requirements	
1	The prototype mount can hold the probe and iPhone securely in a position where the probe can scan.
2	The prototype scanning device can move in x and z directions and rotate about y axis.
3	The patient must be able to put their hand in the water bath comfortably.
4	The probe and iPhone should be easily inserted and removed.
5	The prototype program can piece together images from frames taken from butterfly probe.
6	The prototype program can track position and angle of the probe to piece together images.
7	The transversal mechanism must disengage if met with resistance (safety).

TABLE 3
SPECIFICATIONS

	Specifications	Method of Evaluation
1	Apparatus shouldn't take up an area greater than 2ft^2	Measure length/width with ruler
2	Mount can withstand 3 lbs (force of putting in the butterfly and the weight of butterfly and phone resting on mount)	The force will be evaluated using NX finite element analysis.
3	The Butterfly probe should be able to rotate ±10 degrees about the y-axis	The angle will be measured using a protractor.
4	The Butterfly probe can move at least 6 inches from starting position in the x and z	The distance will be measured using a scale.
5	The Butterfly probe can be moved in the x and z direction with a position accuracy of +/- 0.04 in.	The position accuracy will be measured using a scale or calipers.
6	The Butterfly probe can be angled around the y axis with an accuracy of +/- 1 degree.	The angle accuracy will be measured using an angle finder.
7	The maximum scan time of the tendon should be less than 60 seconds.	The scan time will be measured with a timer.

CONCEPTS

Apparatus-movement Concept Selection	1. Baseline 	2. 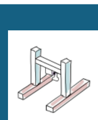	3. 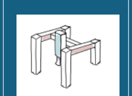	4. 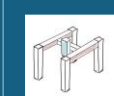
Meets Function	0	+	+	+
Ease of build/assembly	0	+	+	++
Ease of Use	0	+	-	+
Space Requirements	0	+	-	+
Systems Integration	0	++	0	++
Totals:	0	6	0	7

Figure 2. Pugh Matrix of Top Concepts

Figure 2 shows the top concepts of the frame for the apparatus. The baseline is a prototype by Dr. Ketonis and Dr. Loiselle where the probe is moved in the x direction by a stepper motor and belt. Concept 2 differs where the x motion is driven from the bottom and two posts move on the track. Concept 3 has four posts with slanted crossbars that provide the x motion and a separate carriage provides the z motion. Concept 4 is similar to Concept 3; however, the top bars are not slanted and are horizontal and still has the z motion provided by a separate carriage.

Concept 4 was chosen for the movement selection because while the second and third designs have the structure to prevent displacement in the z-direction that the baseline design exhibits, the last design scored the highest in terms of ease of build/assembly.

MECHANICAL ANALYSIS

FATIGUE ANALYSIS

Fatigue analysis is important as it predicts the lifespan of materials that experience cyclical loading so engineers know when that material will fail. While fatigue isn't the main concern regarding the project, a fatigue analysis using the Stress-Life Method was conducted to investigate the lifespan of one of the screws made of alloy steel that secure the stepper motor for the z assembly. This was done by first making an estimate of the endurance limit based on the ultimate strength of alloy steel being 170 kpsi [1] and using Eqn. 1:

$$S_e' = 0.5S_{UT} \quad S_{UT} \leq 200\ kpsi \tag{1}$$
$$S_e' = 85\ kpsi$$

Modification factors based on application are then applied to the initial estimate using Eqn. 2 to compute the endurance limit S_e [2]:

$$S_e = k_a k_b k_c k_d k_e k_f S_e' \tag{2}$$
$$S_e = 48\ kpsi$$

The surface condition modification factor k_a refers to the polish/surface and was calculated to be 0.69 using Eqn. 3:

$$k_a = aS_{UT}^b \tag{3}$$

Where a is 2.70 and b is -0.265 given that the surface finish is under the machined or cold-drawn category.

The size modification factor k_b refers to if it is a square or round sample and was calculated to be 1.1 using Eqn 4:

$$k_b = \left(\frac{d}{0.3}\right)^{-0.107} \quad 0.11 \leq d \leq 2\ in \tag{4}$$

Where diameter d is 0.118 in of a non-rotating specimen.

The load modification factor k_c was taken to be 1 as the sample is loaded where bending is the dominant load type.

The temperature modification factor k_d refers to non-linear temperature effects and was calculated to be 0.98 using Eqn. 5:

$$k_d = 0.975 + 0.432(10^{-3})T_F - 0.115(10^{-5})T_F^2 + 0.104(10^{-8})T_F^3 - 0.595(10^{-12})T_F^4 \tag{5}$$

Where T_F is taken to be 20 °C (room temperature).

The reliability factor k_e refers to the scatter in the data as mean values are used to produce curve fits assuming a standard deviation of 8%. The reliability percent was taken to be 99.9% and k_e was calculated to be 0.753 using Eqn. 6:

$$k_e = 1 - 0.08z_a \tag{6}$$

Where z_a is the transformation variate of 3.091.

The miscellaneous-effects modification factor k_f was taken to be 1 as it refers to local knowledge that is unknown.

To determine if the screw will fail due to fatigue, the screw was analyzed using the Soderberg (Eqn. 7 and Eqn. 8) and Modified Goodman Criterion (Eqn. 9 and Eqn. 10).

The Soderberg Criterion uses yield strength where S_y is 70 kpsi and states fatigue can occur when:

$$\frac{S_a}{S_e} + \frac{S_m}{S_y} \geq 1 \ and\ S_e \leq \frac{S_a}{1 - \frac{S_m}{S_y}} \tag{7,8}$$

The Modified Goodman Criterion uses tensile strength and states fatigue can occur when:

$$\frac{S_a}{S_e} + \frac{S_m}{S_{UT}} \geq 1 \, and \, S_e \leq \frac{S_a}{1 - \frac{S_m}{S_{UT}}} \tag{9,10}$$

Both criteria use S_a (Eqn. 11) and S_m (Eqn. 12) to determine if fatigue will occur. S_a was calculated to be $2.5(10^{-5})$ kpsi and S_m was calculated to be $4.5(10^{-5})$ kpsi.

$$S_a = \left|\frac{S_{max} - S_{min}}{2}\right| \tag{11}$$

$$S_m = \frac{S_{max} + S_{min}}{2} \tag{12}$$

Where S_{max} is the maximum stress that is applied to the screw based on the weight of the z assembly and stepper motor and was calculated to be 70 psi. S_{min} is the minimum stress that is applied to the screw based on just the weight of the stepper motor and was calculated to be 20 psi. The cross-sectional area of the screw was used to calculate the maximum and minimum stresses.

The results of both the Soderberg Criterion and the Modified Goodman Criterion is that fatigue will not occur.

The results of the Soderberg Criterion are:

$$1.2(10^{-6}) \geq 1 \, and \, 48 \leq 2.5(10^{-5}) \tag{7,8}$$

Which shows that failure will not occur by magnitudes of at least 10^5.

Similarly, the results of the Modified Goodman Criterion are:

$$7.9(10^{-7}) \geq 1 \, and \, 48 \leq 2.5(10^{-5}) \tag{9,10}$$

Which shows again that failure will not occur by magnitudes of at least 10^5. This fatigue analysis confirmed that the screws and bolted connections that were chosen can handle the applied loads of the mechanism assembly.

TOLERANCE ANALYSIS

Tolerance analysis is crucial for ensuring proper fit and functionality of the parts within the assembly, ultimately leading to a reliable product. The assembly contains many fasteners, so a tolerance analysis was conducted on the holes mating with the ¼”-20 flat head screws. By analyzing the holes, an acceptable range of variation in hole size can be determined, which can influence the manufacturing process and costs especially if this product were to be mass-produced.

For the tolerance analysis of the holes a clearance fit type (H7/h6) was used to provide a snug fit but can also be freely assembled and disassembled. The maximum diameter of the hole can be calculated using the equation below, where D is the nominal hole size, and ΔD is the tolerance grade for the hole.

$$D_{max} = D + \Delta D \tag{13}$$

The nominal hole size is 0.25-inches, and the tolerance grade for an H7/h6 fit is 0.0006-inches, as cited in Shigley’s [2]. Given these values, the maximum hole diameter was determined to be 0.2506-inches. The minimum diameter of the hole must be equal to that of the nominal diameter, which is 0.2500-inches. For a class 3A ¼”-20 fastener, the maximum diameter is 0.2500-inches, and the minimum diameter is 0.2419-inches [2]. These values describe the maximum and minimum dimensions required so that the screw will always fit in the hole and providing a locational clearance fit type.

FASTENER TORQUE ANALYSIS

The bolted connections used in this assembly are not permanent fasteners. By analyzing the torque to find the proper bolt torque for these connections, it can be ensured that the connections will behave how they were meant to (as a spring) and will not come undone. As shown in Eqn. 14, the proper bolt torque is based on the bolt condition, class, permanent or nonpermanent connections, and size. The bolt being analyzed is an M3 fastener, class 12.9, non-plated, with a non-permanent application.

$$T = KF_i d \tag{14}$$

The nominal major diameter d is 3mm and the bolt condition K is 0.30 as it is non plated/black finish. The following equations are required to find the proper bolt torque.

$$F_i = 0.75F_p \tag{15}$$

$$F_p = A_t S_p \tag{16}$$

From Shigley’s[2], the tensile stress area A_t is taken to be 5.03mm^2 and the minimum proof strength S_p is 970 MPa. F_p is the proof load calculated to be 4880 N using Eqn. 16 and the preload F_i is computed to be 3660 N using Eqn. 15 as it is a non-permanent application.

By using the equations above, the proper bolt torque is calculated to be 3.3 Nm. This confirms that the bolts will be tight enough as a person can apply more than 3.3 Nm with an Allen wrench.

MATERIAL SELECTION

An integral part of this apparatus is the flexure which is what the probe and mount are attached to. This allows for rotation about the y axis so that the probe can scan multiple angles. In order for this to happen, the flexure must be made of a material that is ductile and will not wear as it is used. Multiple flexure iterations were tested in polylactic acid (PLA) and polyethylene terephthalate glycol (PETG). The flexures printed in PLA were too stiff and would wear at the joints as it was flexed repeatedly. The flexures printed in PETG were more flexible than the PLA but would still wear at the joints as it was flexed.

To solve this problem, the flexure body was printed in PLA but the joints were printed in thermoplastic polyurethane (TPU) as shown in Figure 3. TPU was chosen due to its material properties which include high flexibility, high durability, and resistance to abrasion, chemicals, and oils. The higher flexibility and durability allowed the flexure to flex and rotate more easily without wearing at the joints. This change in material did influence how the flexure worked as a whole as it was found that due to its increased flexibility, the flexure did not hold the probe the same way and the probe was pulling at the TPU. Since the part was printed, changing the infill percentage and infill pattern may give more control over how flexible the joint can be. One potential fix is to print the TPU joints with a higher infill to increase stiffness without losing the durability of the joint.

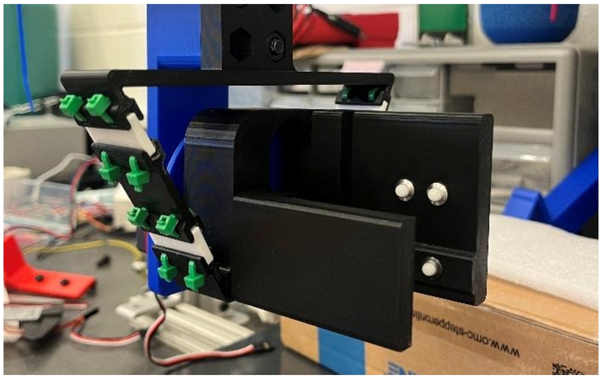

Figure 3. Flexure with TPU joints.

BEARING ANALYSIS

In this assembly, there are many rotating elements which need to be analyzed in order to assess their durability and lifespan. Bearings are typically the first component to fail in rotating machinery, and by calculating bearing life the time of replacement can be predicted, preventing unexpected break downs of the whole system. A common way to assess bearing load life is to determine the C_{10} rating or the basic dynamic load rating, which represents the load a bearing can theoretically handle for a basic rating life of one million revolutions without fatigue damage. The rating defines the life that 90% of a group of identical bearings will exceed under the given load conditions, and the higher the C_{10} rating, the more capable the bearing is of withstanding larger loads for a longer time. The ball bearing life in revolutions, L_{10}, can be determined by utilizing the C_{10} rating in the equation below, where F_D is the desired load.

$$L_{10} = 10^6 \left(\frac{C_{10}}{F_D}\right)^3 \tag{17}$$

The FR188-2RS flanged ball bearing used in the belt drive system for the x-motion has a C_{10} dynamic load rating of 344 N [4]. The desired load can be calculated using Eq. 18, with the applied torque, T, of the stepper motor and the bearing radius, R_b,

$$F_D = \frac{T}{R_b} \tag{18}$$

which are 59 N-cm and ¼-inch, respectively and yields a value of 92.9 N. Using Eqn. 17 and the calculated value for the desired load, the ball bearing life was determined to be 50,772,457 revolutions. The dynamic load rating of this bearing is very high and exceeds that of any load applied in this design allowing the system to have a long lifetime.

SPRING SIZING ANALYSIS

In the flexure, there are plunger pins to locate the probe and phone mount. Two strengths of these pins were ordered for testing, and the result was that the 1.3-3lbs plunger pins held the probe in a more accurate position than the 0.8-2lbs plunger pins. The benefit of the firmer pins was less extraneous movement from the rotation around the y-axis. The lower end of the weaker pins was too weak to reliably hold the probe in the same place, and it was easier for a user to overcome the force of the pins. This could result in less accurate positioning of the probe as compared to the firmer pins.

STRUCTURAL FINITE ELEMENT ANALYSIS

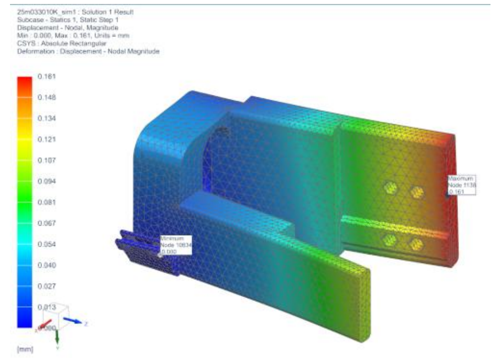

Figure 4. Flexure Simulation Results.

One of the potential issues that was observed during testing was the displacement of the flexure test designs. To evaluate this, the final flexure was used to simulate the displacement of the flexure arms when the probe and phone are being held in the flexure. The preliminary designs had large displacements, so the thickness of the arms was increased, along with the infill of the part. This displacement (Figure 4.) was analyzed to verify that the flexure arms would hold the phone and probe, and that the displacement was within the acceptable limits of the system. The maximum displacement was 0.006 inches. Additionally, the force used in the simulation was on the high end of the force that can be applied by the plunger pins, and the actual force being applied is likely lower. This means that the displacement is within the +/- 0.04 inch tolerance for positional accuracy. This result confirmed that the design changes from the earlier designs were effective, and substantial enough to use the parameters of the final design that was simulated.

FUNDAMENTAL MECHANICAL ANALYSIS

A fundamental statics analysis was conducted on the z-motion and flexure sub-assemblies of the design. This specific study was selected in order to confirm that the torque on the stepper motor that drives the gear is capable of lifting the rack and the probe/flexure mount in the positive z-direction. A free body diagram of the system is shown below in Figure 5.

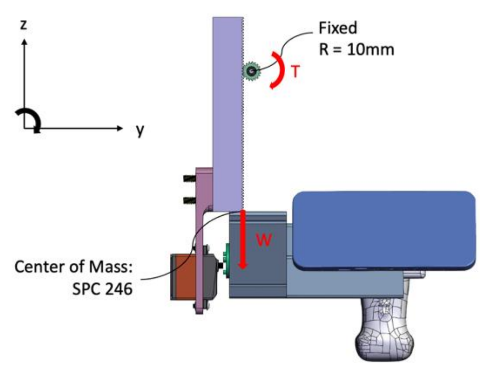

Figure 5. FBD of the rack/pinion and the probe/flexure mount apparatus

The pinion is completely fixed at its center with a radius of 10-mm, and its self-weight can be ignored. A counterweight was added to ensure the center of mass was properly constrained in the y-direction, x-pitch, and z-yaw. The total weight of the rack, mount, phone, probe, and flexure assembly was 0.756 kg. As shown in the free body diagram, the two primary forces acting on the assembly is its own downward gravitational force W, which is equal to the mass multiplied by acceleration due to gravity, and the upward force F_T applied by the rack. Since the minimum torque is desired to begin upward motion, the system must begin in static equilibrium, meaning the net force in the z-direction is zero. Therefore, $F_T = W$.

The pinion generates a tangential force against the rack equivalent to F_T according to Newton's third law of motion. The torque produced by the motor shaft can be found from F_T and the pinion radius, as shown in Eq. 19.

$$T_{min} = F_T R \tag{19}$$

Consequently, the minimum torque required to initiate upward movement of the system, given a pinion radius of 10 mm, was calculated to be 7.42 N-cm. The NEMA 17 stepper motors selected for the design provide a holding torque of 59 N-cm, ensuring they can reliably and confidently drive the system [5].

MANUFACTURING

The primary modes of manufacturing were additive manufacturing in PLA and TPU, and some use of traditional manufacturing techniques for the 8020 aluminum extrusions used for the frame and some threaded rod. CNC machining was also used for creating the angled water bath, which was the only part of the project that purchased shop time with Bill Mildenberger.

Additive manufacturing was used due to the quick iteration time needed for certain parts of the project, such as the flexure for holding and rotating the probe and phone about the y-axis. The additional benefit of the use of 3D printed parts is that the device can be replicated by our sponsor because of their additive manufacturing resources. PLA was used for most of the 3D printed parts due to its low cost and ease of use. TPU was selected for one of the components of the flexure due to its flexibility and durability. The TPU part is the bending joint of the flexure, which needs to have some resistance to reduce extraneous movement while also maintaining alignment of the flexure blades. Additionally, the flexure joints will undergo high repetition of bending, so the material of the joints needs to be durable in this way. During testing, it was found that flexures using PLA at the joints would both prevent the full range of motion and eventually break when used repeatedly. The TPU significantly outperformed the PLA in this way and is also easy to use in additive manufacturing.

The frame of the device is made from 8020 extrusions. These extrusions were chosen because they allow for rapid prototyping by being easy to adjust. An additional benefit of using 8020 aluminum extrusions as the frame is that the channels in the 8020 extrusions could be used for guiding the x-carriage. The 8020 extrusions were cut with a bandsaw, and to create level ends, the ends were milled. Some 8020 parts had holes drilled through them, which was done using a mill to get accurate positioning. One of the rails was made from a standard rectangular extrusion because using an 8020 extrusion in this place would over constrain the design. This piece was machined like the 8020 extrusions were. Threaded rod was used in place of fasteners where the fastener length would have to be over 1.5 inches. The threaded rod was cut to an approximate length using a shear, and then the ends were sanded to remove burrs.

The angled water bath is made from a 1-inch-thick PVC sheet. The guiding idea for selecting PVC was due to it being chemically resistant, since harsh cleaners are used in medical settings. Additionally, PVC is easy to machine and solvent weld. The PVC was cut into four 1"x10"x11" sections using a table saw, adding 1-inch to the nominal length and width dimensions to allow for the machining step to bring the part to its exact dimensions. Next, each section was sanded down on either side to prepare for solvent welding. For the solvent welding steps, we used Bill Mildenberger's help due to the complexity and quickness required to correctly solvent weld large pieces of PVC. Oatey Regular PVC Cement was used for the initial solvent, applied in an even coat to the inner surfaces of the PVC sections, which were then bonded together and secured by clamps while the solvent set for about 20 minutes. To further strengthen the bonds between the PVC layers, methylene chloride, which sets within seconds, was syringed along the edges between each layer and then clamped once more. Once the 4"x10"x11" block of PVC was manufactured, it was CNC machined to its final dimensions using the HAAS Mill.

TABLE 4
BUILD COST ESTIMATE

Category	Cost
Purchased Hardware	$479.11
Purchased Shop Time	$75
3D Print Material Cost	$35.80
Team Member Time	$1,600
Total	$2,189.91

TABLE 5
DEVELOPMENT COST ESTIMATE

Member	Time	Cost
Amanda Lee	144	$14,400
Elizabeth Martin	155	$15,500
Leslii Silveus	172	$17,200
Ava Staub	91.5	$9,150
Total	562.5 hrs	$56,250

If the system was to be scaled to 1000 systems, there are a few changes that would be prioritized to improve the cost and build time. For the frame design, the 8020 extrusions could be replaced by standard rectangular extrusions other than the section used as a channel for the x-carriage. This is because the frame would have a fixed size and fixed points for fastening, and the 8020 was chosen in the original system because it is adjustable. Additionally, the flat 3D printed plates would be changed to machined metal components. These plates are cheap on a small scale with printing, but for larger-scale manufacturing, machined metal would be more cost and time effective. The flexure design would also be adapted to use fasteners or an adhesive to join the TPU and PLA parts. The current method of using zip ties is good for prototyping, but assembly takes more time with the zip ties and current flexure design. Using an adhesive would cut down the build time and would be more cost effective on a larger scale.

TEST PLAN AND RESULTS

TABLE 6
TESTING PLAN OF SPECIFICATIONS

	Specifications	Method of Evaluation	Pass/Fail
1	Apparatus shouldn't take up an area greater than $2ft^2$	The length and width at the most extreme points of the apparatus was measured and recorded.	Passed
2	Mount can withstand 3 lbf (force of putting in the butterfly and the weight of butterfly and phone resting on mount)	The mount was modeled in NX with the correct size and materials. Once the mount was created, an applied force of 3 lbf in the -z direction was applied and used to determine if the mount would fail or not.	Passed
3	The Butterfly probe should be able to rotate ±10 degrees about the y-axis	The angle will be measured using an angle finder at its maximum angles to determine the range of motion.	Passed
4	The Butterfly probe can move at least 6 inches from starting position in the x and z	The initial position of the probe was recorded and then the probe was moved as far as it could go in the x and z. The final position was recorded and the difference from the initial position was measured.	Passed
5	The Butterfly probe can be moved in the x and z direction with a position accuracy of +/- 0.04 in.	An initial starting position was recorded in the x and z direction. Then using the Arduino IDE, the motors in the x and z direction each took one step and the difference was measured.	Passed
6	The Butterfly probe can be angled around the y axis with an accuracy of +/- 1 degree.	The servo was set at an initial position, and using the Arduino IDE, the servo controlling the y was moved 1 degree. This final position was recorded and measured to check its accuracy.	Passed
7	The maximum scan time of the tendon should be less than 60 seconds.	The probe was put in the initial position and a timer was started. The automatic scanning program ran across the whole water bath and the timer was stopped at the end to see the maximum time it takes for the probe to transverse the whole bath.	Passed

TABLE 7
REQUIREMENTS PASS/FAIL

	Requirements	Pass/Fail
1	The prototype mount can hold the probe and iPhone securely in a position where the probe can scan.	Failed – Can hold securely but there is still some displacement in the Z
2	The prototype scanning device can move in x and z directions and rotate about y axis.	Passed
3	The patient must be able to put their hand in the water bath comfortably.	Passed
4	The probe and iPhone should be easily inserted and removed.	Passed
5	The prototype program can piece together images from frames taken from butterfly probe.	Failed – Health Lab took over image processing
6	The prototype program can track position and angle of the probe to piece together images.	Failed – Health Lab took over image processing
7	The transversal mechanism must disengage if met with resistance (safety).	Passed

INTELLECTUAL PROPERTY

This design has many different systems working together to meet its specifications and requirements. However, none of these sub-systems are patentable because they are neither novel nor non-obvious, making the overall design unpatentable.

The x-motion sub-assembly is simply driven using a belt, ball bearings, and a stepper motor, converting rotational motion into linear motion. The concept of this drive system is utilized in many different technologies such as 3D printers, conveyor systems, and CNC machines and typically will have many more components to ensure smoother and more consistent motion. For example, patent WO20050280185A1 (Methods and apparatus for 3D printing) explicitly describes the horizontal positioning to be controlled by a motor-driven belt [6]. Actuators are another type of technology that often incorporates this method of converting rotary motion to linear motion. Patent US20220178424A1 filed by Liftwave Inc., is for a high reduction belt-driven linear actuator [7]. The idea of a belt drive system for the x-motion is not novel and was obvious to us during the concepting stage, failing the patentable criteria.

The rack and pinion sub-system used to drive the z-motion is a very basic and well-known mechanical technology, lacking the novelty required for a patent. Rack and pinions are widely used in applications such as steering systems and lifting mechanisms which many patents in these fields fully disclose. Patent WO1996005453A1 directly patents the rack and pinion drive system, and without a novel modification or non-obvious improvement, a rack and pinion drive system on its own does not meet patentability requirements [8]. Many companies specialize in rack and pinion drive systems, including Atlanta Drive Systems, a world leader offering a large range of mounted pinion technologies [9].

The y-roll servo-driven flexure sub-system is also unpatentable. Flexures are often in technologies used to facilitate displacement and rotary motion of bodies. Patent 11572918 describes a fixed element connected to a mobile element through flexible elements being configured to guide the mobile element according to a rotational movement in a plane [10]. This device offers high angular strokes, up to 45 degrees, which is much more capable then the flexure in this design.

SOCIETAL AND ENVIRONMENTAL IMPLICATIONS

The overall goal of this type of project is to have a positive impact on people's lives. Working with the URMC Health Lab, this project is aimed to improve ultrasound scanning of injured tendons for doctors to assist with treatment plans for patients. The Butterfly iQ3 Ultrasound Probe is useful in emergency situations but does not provide accurate enough imaging in clinical settings due to it being a handheld probe. This mechanism assembly aims to improve that imaging enough so that it can be used in hospitals and provide imaging analysis to aid doctors in patient care. Ultrasound machines are very expensive and an essential piece of equipment for many hospitals so if this mechanism assembly could allow for a cheaper, and just as an accurate option, it could help many people around the world. Due to the timeline of the project, many iterations were tested and in turn that means a lot of plastic waste was created. The majority of the parts in this assembly are 3D printed out of PLA plastic which allows for easy iterating and improving but also leaves behind plastic waste which is very harmful to the environment. While PLA can technically be recycled, very little of it actually is due to it being difficult to separate from other plastics and the lack of infrastructure available that focuses on recycling PLA. One way to reduce the negative impact on the environment from this project is to focus more on collecting waste PLA and recycling it. Another way is to reduce the number of iterations printed and focus more on designing in CAD which would reduce the amount of plastic waste.

RECCOMENDATIONS FOR FUTURE WORK

If given another 6 months to work on this project, there would be additions to the deliverables, and many things on the current design that could be improved. Dr. Ketonis and Dr. Loiselle have a vision for this project to develop into a fully automated system that can cohesively and accurately scan a damaged hand tendon, obtain 3D ultrasound images, calculate the scar tissue volume, and predict the functionality of the patient's tendon. The current design is only capable of performing a partially automated scan which can move in the x and z-directions and rotate about the y-axis.

To get a more representative scan of the entirety of the scar tissue volume in a tendon, rotation of the probe about the x-axis could be incorporated into this design. Also, an interactive touchscreen to control the machine to walk the user through the scanning process rather than button control could improve the electronic aspect of the delivered product. Machine learning algorithms could also be included to predict the functionality of the tendon based on the calculated scar-tissue volume.

Rather than 3D printing the plates, carriages, and the rack/pinion, they would be manufactured using machined metal to increase the durability of the overall design. This would also decrease vibration throughout the system and allow it to move smoother overall. If given access to the app that collects position data from the iPhone along with more time, it would have been ideal to write a program that accurately pieces the ultrasound images together based on position. The current mount provided by UR Health Lab doesn't have as snug of a fit as wanted, so iterations to this design would also be a priority.

ACKNOWLEDGMENTS

The team would like to acknowledge and thank our sponsor Jeff Lillie from UR Health Labs. The team would also like to thank our TA, Sandhya Vaidyanathan, for her help and guidance throughout the project. Additionally, the team would like to thank Alex Prideaux and Sam Kriegsman for help with manufacturing and coding. The team would also like to thank Professor Muir for guidance and advice throughout the project. Lastly, the team wants to thank Bill Mildenberger for assisting in manufacturing and Chris Pratt for assisting in ordering.

REFERENCES

[1] "Alloy Steel Socket Head Screw," McMaster-Carr [Online]. Available: https://www.mcmaster.com/91290A111/

[2] Budynas, R. G., Nisbett, J. K., and Shigley, J. E., 2015, Shigley's Mechanical Engineering Design, McGraw-Hill Education, New York, NY.

[3] "ANSI External Screw Threads Sizes & Tolerances," [Online]. Available: https://www.engineersedge.com/screw_threads_chart.htm

[4] "Uxcell FR188-2RS Flanged Ball 1/4" x 1/2" x 3/16" Double Sealed (GCr15) Chrome Steel Bearings 5pcs," Amazon Prime [Online]. Available: https://www.amazon.com/uxcell-FR188-2RS-Flange-Double-Bearings/dp/B082PSMWXD

[5] “3PCS of Nema 17 Bipolar 59Ncm(83.55oz.in) 2A 42x42x48mm 4 Wires w/ 1m Cable & Connector,” Stepper Online [Online]. Available: https://www.omc-stepperonline.com/3pcs-of-nema-17-bipolar-59ncm-84oz-in-2a-42x48mm-4-wires-w-1m-cable-connector-3-17hs19-2004s1
[6] Russel, D., Hernandez, A., Kinsley, J., and Berlin., A., inventors; Z-Corporation, assignee, 2005, “Methods and apparatus for 3D printing,” International Publication Number 20050280185A1 [Online]. Available: https://patents.google.com/patent/WO2005097476A2/en
[7] Sessions, B., inventor; Liftwave, Inc., assignee, 2022, “High reduction belt-driven linear actuator,” US Patent 20220178424A1 [Online]. Available: https://patents.google.com/patent/US20220178424A1/en
[8] Smithson, A. G., inventor; Alliedsignal Limited, assignee, 1996, “Rack and pinion drive,” International Publication Number 1996005453A1 [Online]. Available: https://patents.google.com/patent/WO1996005453A1/en#patentCitations
[9] “Rack & Pinion Drive Systems,” Atlanta Drive Systems [Online]. Available: https://www.atlantadrives.com/systems.htm?gad_source=1&gbraid=0AAAAAD_NzKj1SRs1qFl6Ykymou1L1D-tD&gclid=CjwKCAjwq7fABhB2EiwAwk-YbCxSFykvooKSJKUuO6m4Eeq_PxzNoxh4DjC_BaFfrVJrbhM0Lo9I-RoCU_oQAvD_BwE
[10] Florent, C., Lionel, K., Philippe, S., inventors; Centre Suisse Delectronique Et Microtechnique Sa Csem, assignee, 2023, “Pivot mechanism with flexible elements for large rotation guiding and pivot assembly comprising of saif pivot mechanism,” US Patent 11572918 [Online]. Available: https://patents.justia.com/patent/11572918

APPENDIX A – CAD ASSEMBLY

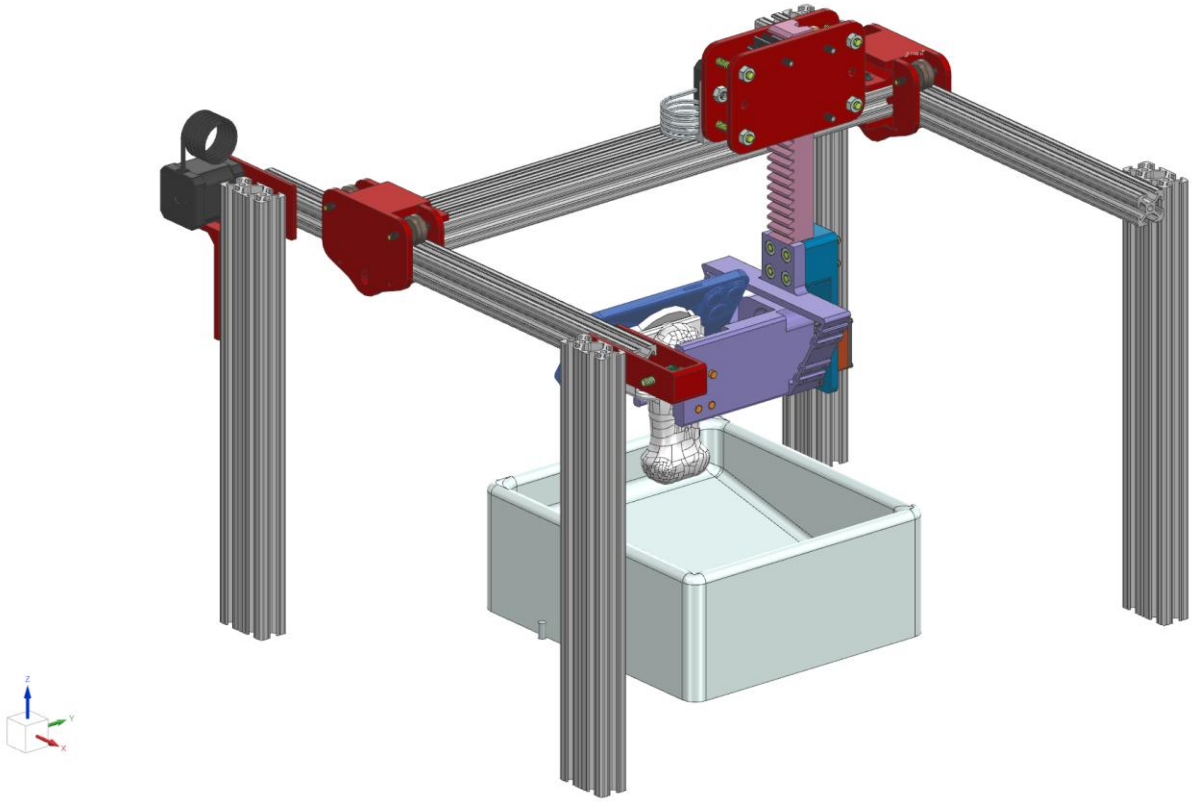

Figure 6. CAD Assembly

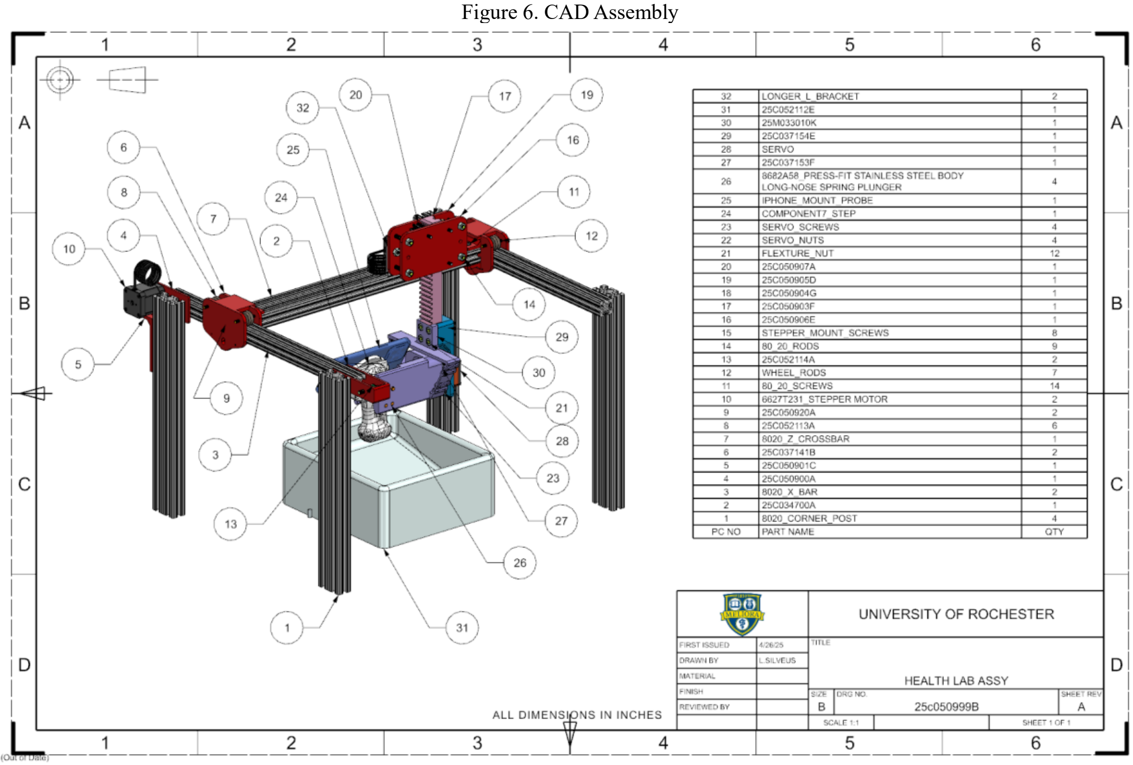

PC NO	PART NAME	QTY
32	LONGER_L_BRACKET	2
31	25C052112E	1
30	25M033010K	1
29	25C037154E	1
28	SERVO	1
27	25C037153F	1
26	8682A58_PRESS-FIT STAINLESS STEEL BODY LONG-NOSE SPRING PLUNGER	4
25	IPHONE_MOUNT_PROBE	1
24	COMPONENT7_STEP	1
23	SERVO_SCREWS	4
22	SERVO_NUTS	4
21	FLEXTURE_NUT	12
20	25C050907A	1
19	25C050905D	1
18	25C050904G	1
17	25C050903F	1
16	25C050906E	1
15	STEPPER_MOUNT_SCREWS	8
14	80_20_RODS	9
13	25C052114A	2
12	WHEEL_RODS	7
11	80_20_SCREWS	14
10	6627T231_STEPPER MOTOR	2
9	25C050920A	2
8	25C052113A	6
7	8020_Z_CROSSBAR	1
6	25C037141B	2
5	25C050901C	1
4	25C050900A	1
3	8020_X_BAR	2
2	25C034700A	1
1	8020_CORNER_POST	4

Sheet "Sheet 1" Work (Out of Date)

Figure 7. Assembly Drawing and BOM

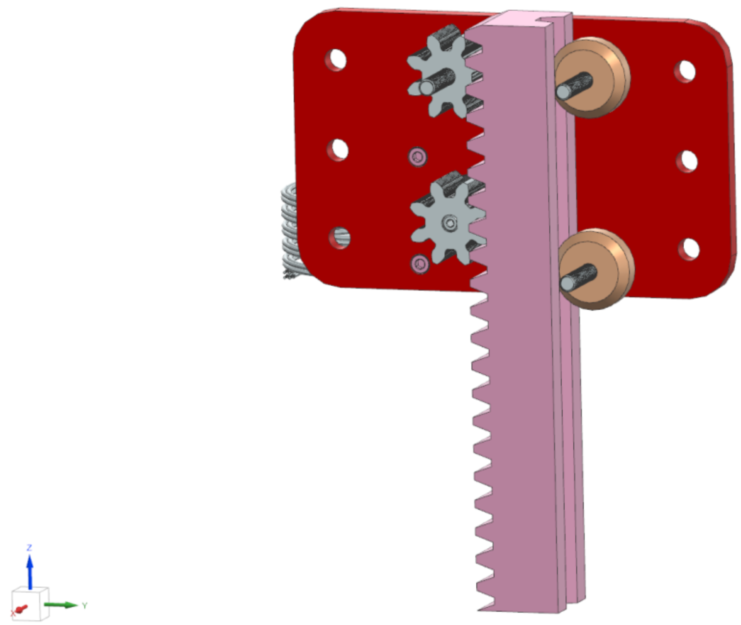

Figure 8. Inner Z Rack

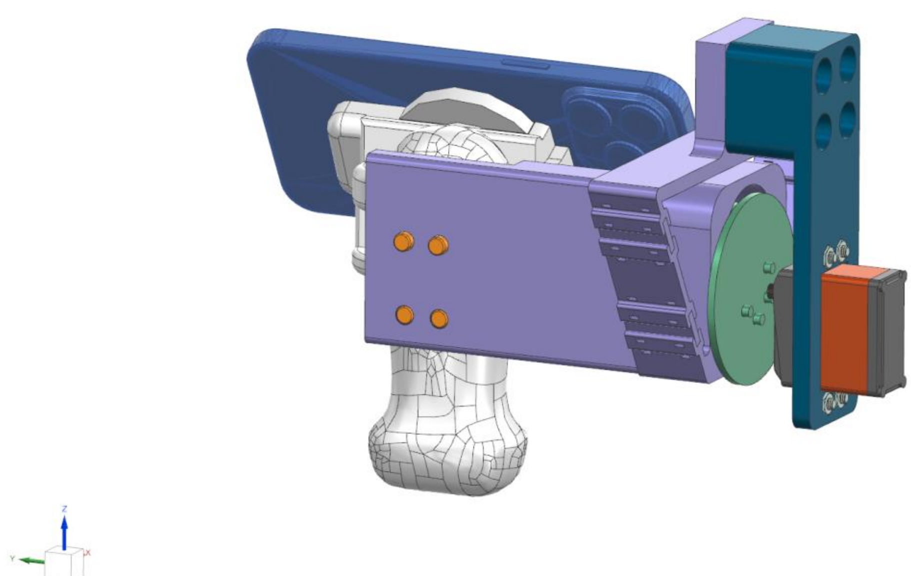

Figure 9. Flexure and Probe Mount

APPENDIX B - FEA

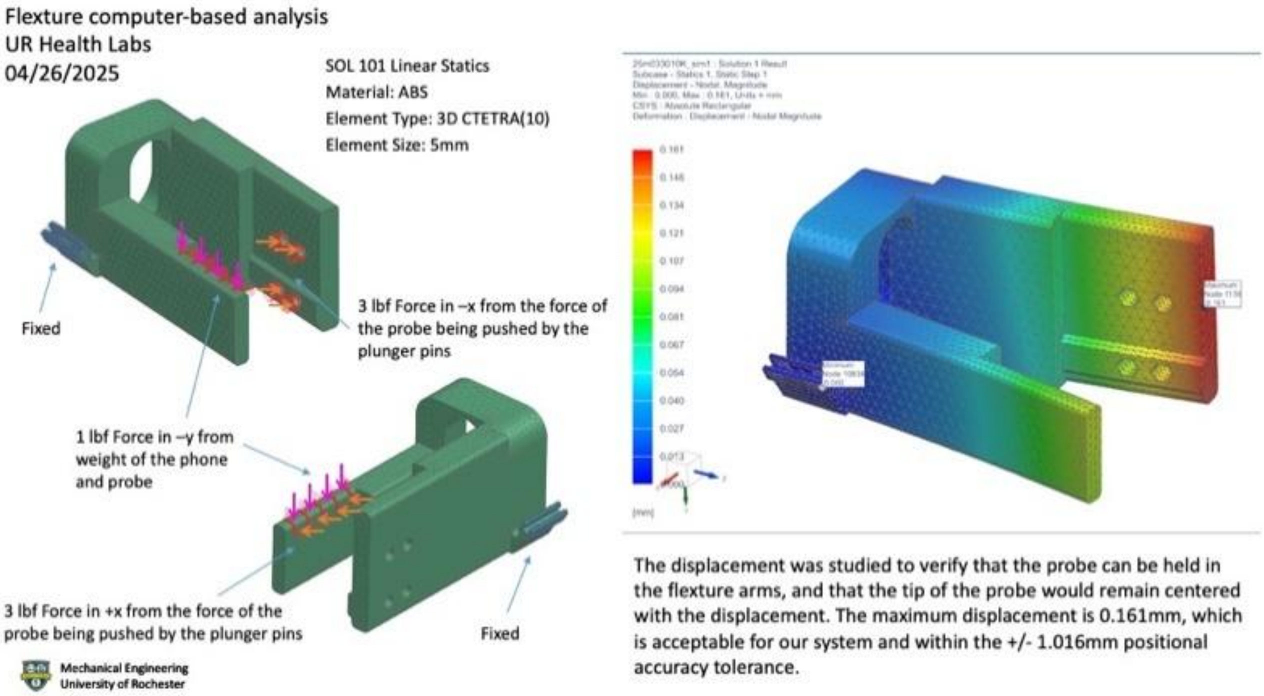

Figure 10. FEA Displacement Analysis

APPENDIX C – CIRCUITS

Circuit Components
Health Lab

Bill of Materials		
Item	quantity	Schematic Designation
Arduino Mega	1	U2
Arduino Uno	1	U1
A4988 Stepper Motor Driver	2	U4,U5
Nema 17 Stepper Motor Bipolar 2A 59Ncm	2	X Stepper Motor, Z Stepper Motor
Push Button	8	S1, S2, S3, S4, S5, S6, S7, S8
10k Ohm Resistors	8	R1, R2, R3, R4, R5, R6, R7, R8
20kg RC Servo High Torque Servo Motor	1	Servo
Adafruit VL6180X Time of Flight Distance Ranging Sensor	1	U3

Mechanical Engineering
University of Rochester

Figure 11. Circuit Bill of Materials

Circuit Components
Health Lab

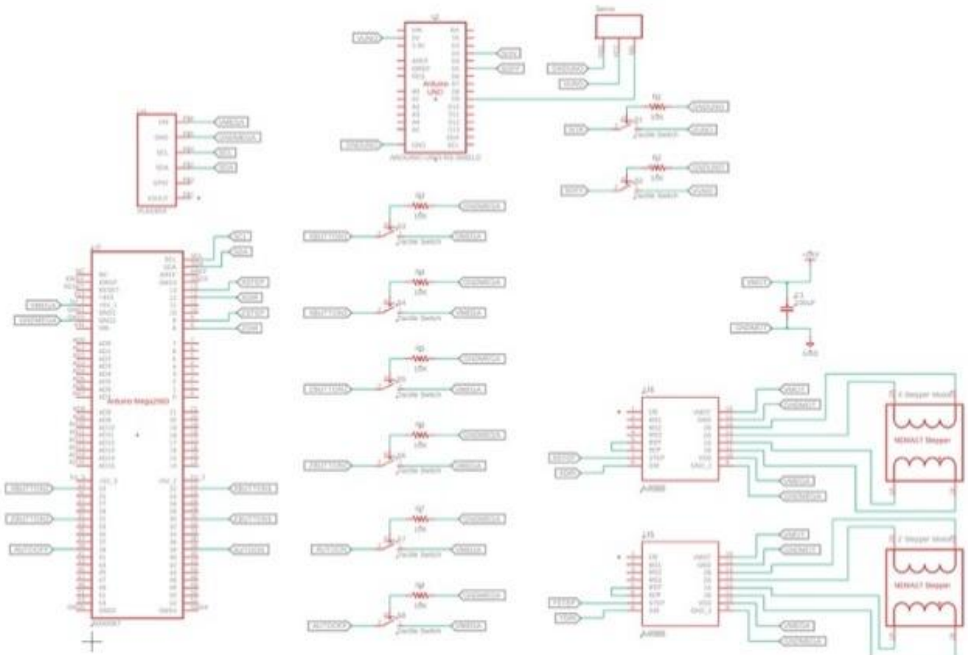

Mechanical Engineering
University of Rochester

Figure 12. Circuit Diagram